

1 **‘Warm Cover’- Precursory ‘Strong Signals’ hidden in the Middle**  
2 **Troposphere for Haze Pollution**

3  
4 **Xiangde Xu<sup>1</sup>, Wenyue Cai<sup>1,2,3</sup>, Tianliang Zhao<sup>4</sup>, Xinfu Qiu<sup>5</sup>, Wenhui Zhu<sup>6</sup>, Chan Sun<sup>1</sup>, Peng Yan<sup>7</sup>,**  
5 **Chunzhu Wang<sup>8</sup>, and Fei Ge<sup>9</sup>**

6 <sup>1</sup>State Key Laboratory of Severe Weather (LASW), Chinese Academy of Meteorological Sciences, Beijing,  
7 China.

8 <sup>2</sup>National Climate Center, China Meteorological Administration, Beijing, China.

9 <sup>3</sup>School of Geographical Science, Nanjing University of Information Science and Technology, Nanjing,  
10 Jiangsu Province, China.

11 <sup>4</sup>Key Laboratory for Aerosol-Cloud-Precipitation of China Meteorological Administration, Nanjing  
12 University of Information Science and Technology, Nanjing, Jiangsu Province, China.

13 <sup>5</sup>School of Applied Meteorology, Nanjing University of Information Science and Technology, Nanjing,  
14 Jiangsu Province, China.

15 <sup>6</sup>Beijing Institute of Applied Meteorology, Beijing, China.

16 <sup>7</sup>Meteorological Observation Center, China Meteorological Administration, Beijing, China.

17 <sup>8</sup>Training Center, China Meteorological Administration, Beijing, China.

18 <sup>9</sup>School of Atmospheric Sciences/Plateau Atmosphere and Environment Key Laboratory of Sichuan  
19 Province/Joint Laboratory of Climate and Environment Change, Chengdu University of Information  
20 Technology, Chengdu, ~~Sichuan~~ Province, China.

删除的内容: Sichuan

21

22

23 **Correspondence:** Wenyue Cai (caiwy@cma.gov.cn) and Tianliang Zhao (tlzhao@nuist.edu.cn)

24

26 **Abstract.** Eastern China (EC), located in the downstream region of Tibetan Plateau (TP), is a large area  
27 with frequent haze pollution. In addition to air pollutant emissions, meteorological conditions were a key  
28 ‘inducement’ for air pollution episodes. Based on the study of the Great Smog of London in 1952 and haze  
29 pollution in EC over recent decades, it is found that the abnormal ‘warm cover’ (air temperature warm  
30 anomalies) in the middle troposphere, as a precursory ‘strong signal’, could connect to severe air pollution  
31 events. The convection and vertical diffusion in the atmospheric boundary layer (ABL) were suppressed by  
32 a relatively stable structure of ‘warm cover’ in the middle troposphere, leading to the ABL height decreases,  
33 which was favourable for the accumulation of air pollutants in the ambient atmosphere. The anomalous  
34 structure of the troposphere’s “warm cover” not only exist in heavy haze pollution on the daily scale, but  
35 also provide seasonal, interannual and interdecadal ‘strong signals’ for frequently occurring regional haze  
36 pollution. It is revealed that a close relationship existed between interannual variations of the TP’s heat  
37 source and the ‘warm cover’ strong-signal in the middle troposphere over EC. The warming TP could lead  
38 to the anomalous ‘warm cover’ in the middle troposphere from the plateau to the downstream EC region  
39 and even the entire East Asian region for air pollution.

删除的内容: o

删除的内容: that has become vulnerable to

删除的内容: of

删除的内容: hidden

删除的内容: were

删除的内容: built

删除的内容: The frequent haze events in EC is connected with a significantly strong ‘warm cover’ in the interdecadal variability. It is also revealed that a close relationship existed between interannual variations of the TP’s heat source and the ‘warm cover’ hidden in the middle troposphere over EC.

## 41 1 Introduction

42 In China, mainly over the region east of 100 °E and south of 40 °N (Tie et al., 2009), PM<sub>2.5</sub> (particulate  
43 matter with an aerodynamic diameter equal to or less than 2.5 μm) has become the primary air pollutant in  
44 winter (Wang, et al., 2017). Therefore, in September 2013, the Chinese government launched the China’s  
45 first air pollution control action plan-‘The Airborne Pollution Prevention and Control Action Plan  
46 (2013-2017)’ (State Council of the People’s Republic of China, 2013). By 2017, about 64% of China’s  
47 cities are still suffering from air pollution, especially Beijing-Tianjin-Hebei region and surrounding areas  
48 (Wang et al., 2019; Miao et al., 2019). Then, in July 2018, the Chinese government launched the second  
49 three-year action plan for air pollution control, the “blue sky defense plan”, which demonstrates China’s  
50 firm determination and new measures for air pollution control (State Council of the People’s Republic of  
51 China, 2018). After the implementation of air pollution control action plans, air quality in many regions in  
52 China has been significantly improved.

删除的内容: the

删除的内容: the

删除的内容: and cities

53 Anthropogenic pollutant emissions and unfavorable meteorological conditions are commonly regarded

73 as two key factors for air pollution (Ding and Liu, 2014; Yim et al., 2014; Zhang et al., 2015). Air  
74 pollutants mainly come from surface emission sources, and most of air pollutants are injected from the  
75 surface to the atmosphere through the atmospheric boundary layer (ABL) (Quan et al., 2020). The ABL  
76 structures are the key meteorological conditions which influences the formation and maintenance of heavy  
77 air pollution episodes (Wang et al., 2015; Cheng et al., 2016; Wang et al., 2016; Tang et al., 2016; Wang et  
78 al., 2019).

删除的内容: haze

删除的内容: with excessive concentrations of PM<sub>2.5</sub>

删除的内容: ,

删除的内容: The thermodynamic structures in atmospheric boundary layer and the free troposphere

删除的内容:

删除的内容: influencing

79 Most of the previous studies focused on exploring the impact on the heavy air pollution in Eastern  
80 China (EC) from the meteorological conditions in ABL. However, the thermodynamic and dynamic  
81 structures of free troposphere can affect the meteorological conditions in ABL (Cai et al., 2020). The  
82 convection and diffusion in the ABL are suppressed by a relatively stable structure in the middle  
83 troposphere, leading to the ABL height decreases, which was favourable for the formation and persistence  
84 of heavy air pollution (Quan et al., 2013; Wang et al., 2015; Cai et al., 2020).

删除的内容: atmospheric boundary layer (

删除的内容:)

85 This study investigated whether the thermodynamic structure of the troposphere and its intensity  
86 changes can be used as a "strong warning signal" for the changes of PM<sub>2.5</sub> concentrations in heavy air  
87 pollution, and whether this strong signal exists in the time scales of seasonal, interannual and interdecadal  
88 changes. In order to explore the interaction between the free troposphere and the ABL, and the impact on  
89 the heavy air pollution in EC, this study extended the meteorological conditions for heavy air pollution  
90 from the boundary layer to the middle troposphere. We identify a precursory 'strong signals' hidden in the  
91 free troposphere for frequent haze pollution in winter in EC.

删除的内容: the structure of atmospheric thermodynamics in the troposphere and its intensity variation could act as a 'strong forewarning signal' for surface PM<sub>2.5</sub> concentration variations in heavy air pollution.

删除的内容: atmospheric boundary layer

删除的内容: Eastern China

删除的内容: Eastern China

## 93 2 Data and methods

94 The data used in this study included NCEP/NCAR and ERA-Interim reanalysis data of meteorology, as

删除的内容:

118 well as data of surface PM<sub>2.5</sub> concentration measurement, air temperature observation and L-band sounding,  
119 as briefly described as follows:

120 The monthly NCEP/NCAR reanalysis data of meteorology with horizontal resolution of 2.5° of  
121 1960-2019 were obtained from the U.S. National Center for Environmental Protection (NCEP,  
122 <https://www.esrl.noaa.gov/>).

123 The daily and monthly ERA-Interim reanalysis data of meteorology with horizontal resolution of 0.75°  
124 were derived from the European Center for Medium-range Weather Forecasts (ECMWF,  
125 <https://www.ecmwf.int/>), including air temperature, geopotential height, humidity, wind field and vertical  
126 velocity.

127 The hourly PM<sub>2.5</sub> concentration data during 2013-2019 were collected from the national air quality  
128 monitoring network operated by the Ministry of Ecology and Environment [the People's Republic](#) of China  
129 (<http://www.mee.gov.cn/>). In addition, we categorized air pollution levels with the surface PM<sub>2.5</sub>  
130 concentrations based on the National Ambient Air Quality Standards of China (HJ633-2012) released by  
131 the Ministry of Ecology and Environment in 2012 as shown in Table 1.

132 We also used the monthly air temperature of surface observation data during 1960-2014 from 58  
133 meteorological observation stations in the plateau area with an altitude above 3000 meters, which were  
134 archived from the China Meteorological Information Center (<http://data.cma.cn/>).

135 Furthermore, the L-band sounding 'seconds-level' data of Beijing from 2010 to 2019 to were used to  
136 calculate the height of ABL (Liu and Liang, 2010). The height of ABL top is characterized by the L-band  
137 sounding observations at 20:00 (local time is used for this paper). The L-band sounding 'seconds-level'  
138 data has been undergone the quality control before analysis (Zhu et al., 2018), and interpolation was  
139 implemented in a vertical direction at an interval of 2 hPa. The L-band detection data provided by the

删除的内容: for

删除的内容:

删除的内容: , etc

删除的内容: <http://cdc.cma.gov.cn/>

删除的内容: the site

删除的内容: atmospheric boundary layer

删除的内容: ABL,

删除的内容: 5

删除的内容: -

删除的内容: (Zhu et al., 2018)

151 [China Meteorological Information Center](http://data.cma.cn/) (<http://data.cma.cn/>) contains several automatic observation  
 152 meteorological elements with time resolution of 1.2 s and vertical resolution of 8 m. More detail  
 153 information can be found in Li et al. (2009) and Cai et al. (2014).

删除的内容: the Meteorological Observation Network  
 删除的内容: <http://cdc.cma.gov.cn/>

154 **Table 1. Air pollution degrees categorized with surface PM<sub>2.5</sub> concentrations**

Air pollution degrees	PM <sub>2.5</sub> concentration <u>ranges</u>
‘less-serious’ pollution	75 μg·m <sup>-3</sup> < PM <sub>2.5</sub> ≤ 115 μg·m <sup>-3</sup>
‘serious’ pollution	115 μg·m <sup>-3</sup> < PM <sub>2.5</sub> ≤ 150 μg·m <sup>-3</sup>
‘more-serious’ pollution	150 μg·m <sup>-3</sup> < PM <sub>2.5</sub> ≤ 250 μg·m <sup>-3</sup>
‘most-serious’ pollution	PM <sub>2.5</sub> > 250 μg·m <sup>-3</sup>

带格式的: 居中

155  
 156 **3 Results**

157 **3.1 A precursory ‘strong signal’ of ‘warm cover’ in the middle troposphere**

158 In February 2014, a rarely persistent air pollution weather process occurred in EC with severe air pollution  
 159 in more than 50 cities, with an impact area of 2.07 million km<sup>2</sup>. In the Beijing area during February 20–26,  
 160 2014 the regional average PM<sub>2.5</sub> concentration exceed the ‘most-serious’ air pollution level, and with a  
 161 peak value of up to 456 μg m<sup>-3</sup>. In addition, the Great Smog of London in 1952 was attributed to the  
 162 long-lasting and heavy haze pollution, under the influence of certain weather systems (Whittaker et al.,  
 163 2004). To find the precursory ‘strong signals’ hidden in meteorology for heavy air pollution events, we  
 164 retrieved the three-dimensional atmospheric dynamic, and thermal structures during December in 1952 as  
 165 well as February in 2014 by analyzing vertical anomalies of meteorology. There were high-pressure  
 166 systems moved to London as well as Beijing and stagnated over both areas at 500 hPa geopotential  
 167 height anomalies, as shown in Figs. 1a and 1b. During the heavy air pollution events, a high-pressure  
 168 system over London as well as Beijing gradually strengthened (Figs. 1c and 1d), and the middle  
 169 troposphere was characterized by a ‘warm cover’ with ‘upper warming and bottom cooling’ anomalies in  
 170 vertical structure of air temperature (Figs. 1e and 1f).

删除的内容: square kilometers  
 带格式的: 上标  
 删除的内容: In the Beijing area and surroundings over North China Plain during February 18–27, 2014, the regional average PM<sub>2.5</sub> concentrations reached up to 250 μg m<sup>-3</sup> for the prolong heavy air pollution. T  
 删除的内容: the accumulation of low-level smoke and sulfur-dioxide pollutants  
 删除的内容: of the  
 删除的内容: both  
 删除的内容: s  
 删除的内容: the  
 删除的内容: -  
 删除的内容: -  
 删除的内容: Prior to  
 删除的内容: -  
 删除的内容: -  
 删除的内容: , i.e. a  
 删除的内容: -

195 By comparing Figs. 1a and 1b, we found that two persistent heavy air pollution events occurred during  
196 the maintenance stage of stable high pressure system. During stagnation of the blocking high pressure  
197 system, the strength of the center of the geopotential height anomalies in the stable maintenance region of  
198 the blocking exhibited a synchronous response to the ‘warm cover’ above areas (Figs. 1c–1f). It can be seen  
199 that the local atmospheric thermal structure is significantly modulated by the persistent large-scale  
200 anomalous circulation. The ‘subsidence-induced air temperature inversion’ effect of the blocking high  
201 pressure system continuously strengthened the ‘warm cover’ structure in the middle troposphere, which  
202 suppressed the vertical diffusion capacity in the atmosphere (Cai et al., 2020). Moreover, it was obvious  
203 that ‘strong signals’ arising from the thick ‘warm cover’ persisted during the abnormal air-pollution episode  
204 during December 5–9, 1952 in London as well as February 21–26, 2014 in Beijing. It is worth pointing out  
205 that the bottom edge of ‘warm cover’ in the free troposphere declined day-by-day. During the heavy  
206 pollution incident, the ‘warm cover’ dropped to 900 hPa (Figs. 1g and 1h). The above analysis shows that  
207 in the ABL over London during December 5–9, 1952 and Beijing during February 21–26, 2014, the  
208 inversion layer height decreased, which made the ABL structure stable for accumulation of air pollutants.  
209 The deep ‘warm cover’ structures in the middle troposphere acted as a precursory ‘strong signal’ of the  
210 Great Smog of London and Beijing’s heavy air pollution.

删除的内容: Fig.

删除的内容: two long heavy air pollution

删除的内容:

删除的内容: 3D dynamical and thermodynamical structures were

删除的内容: (

删除的内容: (

删除的内容: )

删除的内容: The air temperature inversion

删除的内容: -

删除的内容: ,

删除的内容: upper air

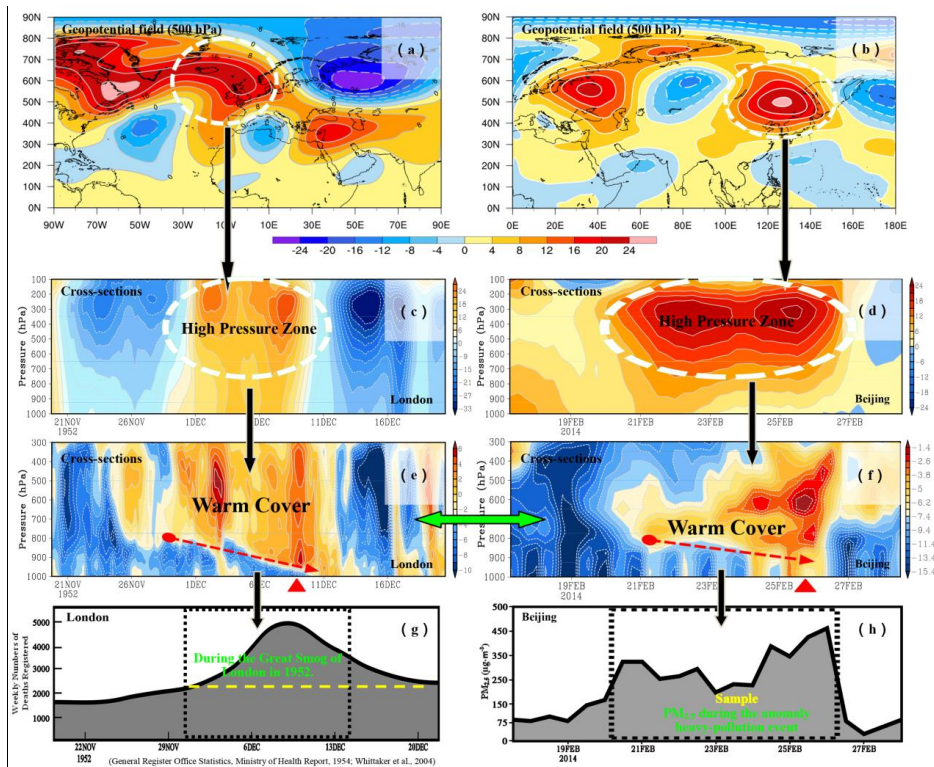
删除的内容: ‘subsidence

删除的内容: of air temperature in the high pressure system

删除的内容: and the inversion layer ABL

删除的内容: atmospheric

删除的内容: aerosols



232  
 233 **Figure 1.** Dynamical and thermodynamical structures and air pollution variations: (a) geopotential height anomalies (unit: dagpm) at 500 hPa during December 5-9, 1952 for the Great Smog of London, (b) the same as (a) but during February 21-26,  
 234  
 235 2014. (c) Time-vertical cross-sections of the geopotential height anomalies (unit: dagpm) in the high pressure area (50-70 N;  
 236 20°W -10°E) during November 20 to December 20, 1952, (d) the same as (c) but in the high pressure area (40-63 N;  
 237 115-138°E) during February 17-28, 2014. (e) Time-vertical cross-sections of air temperature anomalies (unit: °C) over  
 238 London (the Red dotted arrow shows the bottom edge of the ‘warm cover’ during the Great Smog in London) during  
 239 November 20 to December 20, 1952, (f) the same as (e) but during the heavy pollution in February 2014 over Beijing. (g)  
 240 Weekly death rate in London prior to, during and after the 1952 pollution episode (General Register Office Statistics,  
 241 Ministry of Health Report, 1954; Whittaker et al., 2004). (h) The variation of surface PM<sub>2.5</sub> concentrations (units: μg·m<sup>-3</sup>)  
 242 during the heavy pollution in February 2014 over Beijing.

243

244 **3.2 Effect of ‘Warm Cover’ in the free troposphere on ABL and surface PM<sub>2.5</sub> variations**

245 During five heavy air pollution episodes over Beijing in December 2015 and 2016 the vertical structures of  
 246 air temperature anomalies presented the ‘warm cover’ structure in the free troposphere (see Fig. S1).

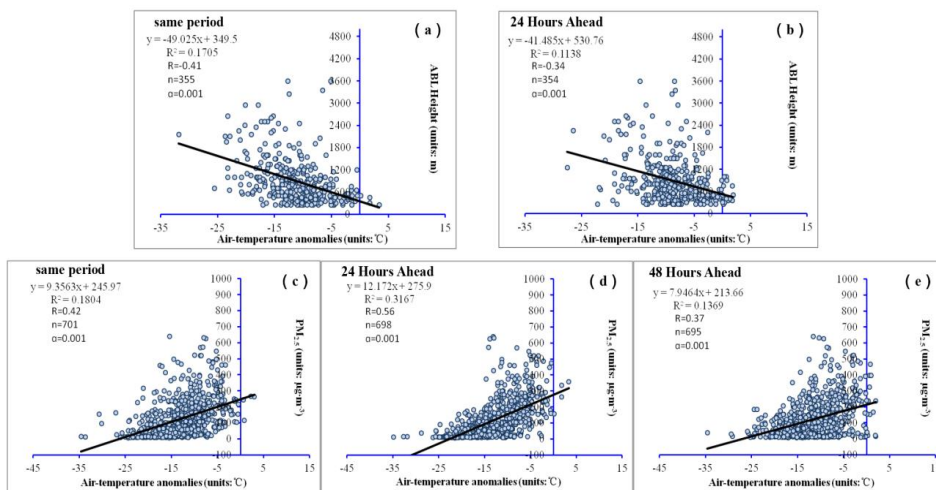
- 删除的内容: 3
- 删除的内容: d
- 删除的内容: -
- 删除的内容: .
- 删除的内容: Geopotential
- 删除的内容: -
- 删除的内容: p
- 删除的内容: to
- 删除的内容: (during
- 删除的内容: ; unit: dagpm)
- 删除的内容: to
- 删除的内容: (c)
- 删除的内容: zone
- 删除的内容: -
- 删除的内容: zone
- 删除的内容: unit: °C, here
- 删除的内容: .
- 删除的内容:
- 删除的内容: and boundary layer with aerosol

267 During winter 2014-2017, Figs. 2a and 2b demonstrated the significant negative correlations between the  
 268 height of the ABL and air temperature anomalies over same period and 24 hours ahead in Beijing, and the  
 269 correlation coefficients were 0.41 and 0.34 (99.9% confidence level), reflecting that the ‘warm cover’  
 270 structure hidden in the middle troposphere with significant ‘strong-signal’ features is of persistent  
 271 premonitory significance for the heavy pollution episodes. Figs. 2c-2e presented the significant positive  
 272 correlations between PM<sub>2.5</sub> concentrations and air temperature anomalies over same period and 24, 48  
 273 hours ahead in Beijing, and the correlation coefficients were 0.42, 0.56 and 0.37 (99.9% confidence level).  
 274 Based on the above mentioned results, air temperature anomalies over 24 and 48 hours ahead could also  
 275 be reflected that ‘warm cover’ hidden in the middle troposphere could be regarded as the precursory  
 276 ‘strong-signal’ for air pollution change. Furthermore, such a ‘stable’ structure also restricted the vertical  
 277 transport of moist air from the lower to the middle troposphere for forming secondary aerosols, which  
 278 could dominate PM<sub>2.5</sub> concentrations in air pollution over China (Huang et al., 2014; Tan et al., 2015).

删除的内容: Fig.  
 删除的内容:  
 删除的内容: passing 0.001 confidence degree  
 删除的内容: atmospheric boundary layer (  
 删除的内容:)

删除的内容: passing 0.001 confidence degree

删除的内容: A



删除的内容: (a)  
 删除的内容: atmospheric boundary layer (  
 删除的内容:)  
 删除的内容: -  
 删除的内容: .  
 删除的内容: -  
 删除的内容: in Beijing during winter 2014-2017  
 删除的内容: -  
 删除的内容: -  
 删除的内容: -  
 删除的内容: in Beijing during winter 2014-2017

279 **Figure 2.** The correlations between ABL height and air temperature anomalies in Beijing during winter 2014-2017, (a) same  
 280 period, at 800 hPa; (b) 24 hours ahead, at 650 hPa. The correlations between PM<sub>2.5</sub> concentration and air temperature  
 281 anomalies in Beijing during winter 2014-2017, (c) same period, at 850 hPa; (d) 24 hours ahead, at 800 hPa; (e) 48 hours  
 282 ahead, at 724 hPa.



307

308 **3.3 Changes of the ‘warm cover’ structure in the middle troposphere**

309 The ‘warm cover’ structure of air temperature anomalies in the middle troposphere indicated the  
310 intensification of heavy air pollution. The ‘warm cover’ structure is a precursory ‘strong signal’ for the  
311 frequent occurrence of regional haze events. The air pollution in EC exhibited the significant seasonal  
312 variations. Our study revealed that existed seasonal differences of the thermal structures in the atmosphere  
313 over EC. In spring (Figs. 3a, and 3e) and summer (Figs. 3b, and 3f), the middle troposphere was  
314 characterized by a ‘upper cooling and bottom warming’ vertical structure for less air pollution. When the  
315 autumn (Figs. 3c and 3g) and winter (Figs. 3d and 3h) arrived, the middle troposphere was characterized by  
316 a ‘upper warming and bottom cooling’ vertical structure, which intensified the air pollution. In autumn,  
317 atmospheric thermal structure over EC was marked with a transition between summer and winter (Fig. 3c).  
318 The atmosphere condition reversed in winter, a large-scale anomalous air temperature pattern of ‘upper  
319 warming and bottom cooling’ in the middle troposphere appeared from the plateau to downstream EC  
320 region and even the entire East Asian region (Fig. 3d). The structure of ‘warm cover’ in winter was much  
321 stronger than that in autumn, and its height of the former was much lower than that of the latter. Therefore,  
322 the intensity of air pollution over EC during winter is significantly higher than other seasons (Fig. 3h).

323 From the perspective of interdecadal variations, our study revealed a close relationship between the  
324 frequent occurrence of haze events in EC and the atmospheric thermal structure in the eastern Tibetan  
325 Plateau (TP). Furthermore, the thermal structures of the troposphere exhibited the distinct interdecadal  
326 variations (Figs. 4a-4c). A cooling structure was identified in the wintertime air temperature anomalies over  
327 the east region of TP during 1961–1980 (Fig. 4a); the upper level of the eastern TP during 1981–2000  
328 showed a ‘upper cooling and bottom warming’ vertical structure (Fig. 4b). The interdecadal changes of  
329 vertical structure reversed during 2001–2018 with a significant ‘warm cover’ (Fig. 4c). The years of 2001–

删除的内容: Eastern China (

删除的内容:)

删除的内容: in terms

删除的内容: .

删除的内容: .

删除的内容: (Fig. 3c, g) or

删除的内容: . 3d,

删除的内容: TP

338 2018 witnessed the highest frequency of haze days (Fig. 4f), and 1981–2000 saw a middle-level occurrence  
339 of haze days (Fig. 4e), while the lowest frequency of haze days occurred during 1961–1980 (Fig. 4d).

340 The concept of variations of the tropospheric ‘warm cover’ has been proposed in this work. Under the  
341 background of climate change, it is worth considering whether the variational tendency of the structure of  
342 the plateau’s heat source induces variations of the tropospheric thermal structure in downstream areas of the  
343 Plateau, leading to the interdecadal variations of the frequency of haze events seen in Eastern China since  
344 the 21th century. Thermal anomalies of the TP also play an important role in the variations of the frequency  
345 of haze events in EC apart from the anthropogenic pollutant emission related to the rapid industrialization  
346 of China. The observational and modeling studies have demonstrated that the interannual variations in the  
347 thermal forcing of TP are positively correlated with the incidences of wintertime haze over EC (Xu et al.,  
348 2016). The TP induced changes in atmospheric circulation, increasing atmospheric stability and driving  
349 frequent haze events in EC (Xu et al., 2016). In this study, the data analysis concerning the interannual  
350 variations of the TP’s apparent heat source and air temperature in wintertime at the TP with the altitudes  
351 above 3000 meters showed that since the 1960s the heat source in areas vulnerable to TP climate change  
352 strengthen continuously as the surface temperature increased (Fig. 5a). Furthermore, the TP’s apparent heat  
353 and air temperature of the middle troposphere over EC presented the significant positive correlation passing  
354 (90% confidence level), which is similar to ‘warm cover’ structures (Fig. 5b). Therefore, we considered that  
355 the ‘warm cover’ change in the middle troposphere over EC was closely related to TP’s apparent heat and  
356 the surface temperature. The TP induced changes in thermodynamic structure of atmospheric provided  
357 favorable climatic backgrounds driving air pollution events in EC.

删除的内容: interdecadal

删除的内容: in

删除的内容: and whether these could also

删除的内容: the

删除的内容: (

删除的内容: )

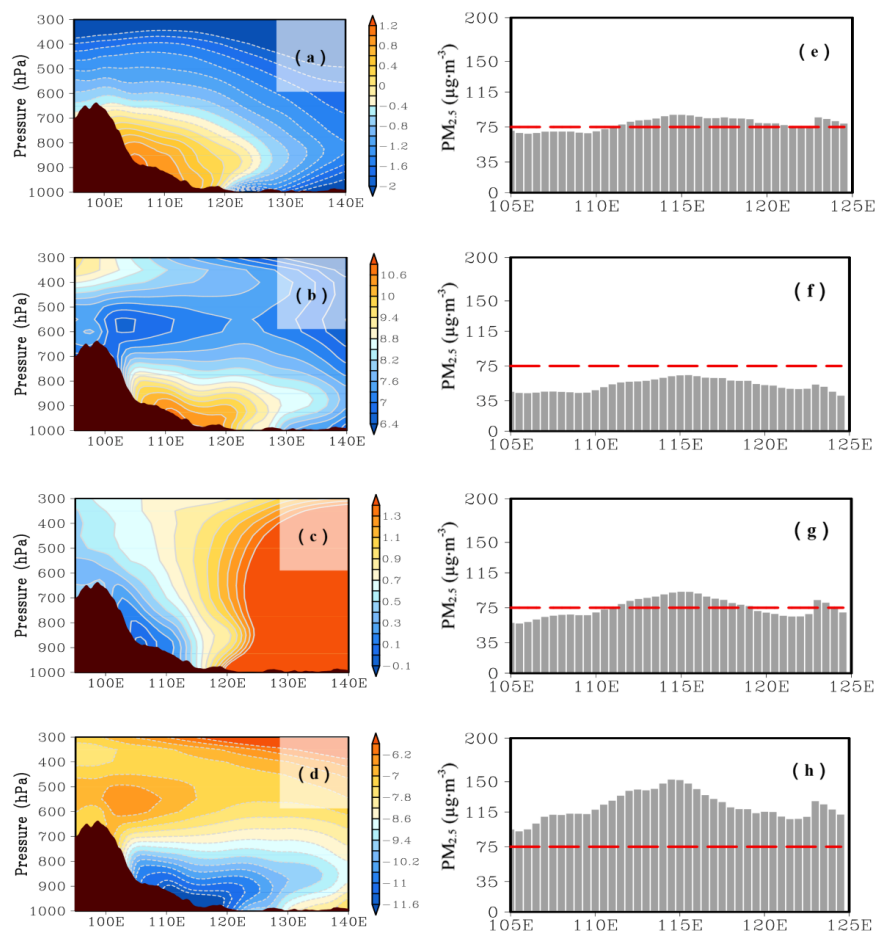
删除的内容: the significant positive

删除的内容: characteristic

删除的内容: (

删除的内容: )

删除的内容: It is worth considering whether the variations of the plateau’s heat structures could lead to the interdecadal variations of the ‘warm cover’ in the troposphere for the frequent occurrence of haze in EC since the 21st20th century (Fig. 4c, f). By analyzing TP’s apparent heat source (Q1) and air temperature observed at meteorological stations over the TP in the winters during 1960-2014 (Fig. 5a, b), we found that the ‘warm cover’ changes in the middle troposphere over EC and even in East Asia was closely related to the surface temperature and TP’s apparent heat.



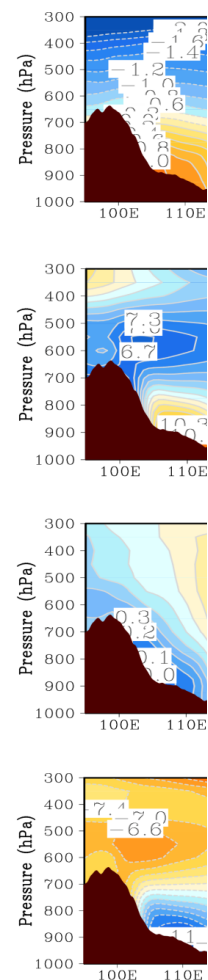
386

387

388

**Figure 3.** Vertical cross sections of (a-d) air temperature anomalies (unit: °C) and (e-h) the PM<sub>2.5</sub> concentrations (unit: µg·m<sup>-3</sup>) averaged along 25-40°N in spring (a, e), summer (b, f), autumn (c, g), winter (d, h) from 2013 to 2018.

带格式的: 字体: Times New Roman



删除的内容:

删除的内容: C

删除的内容: ,

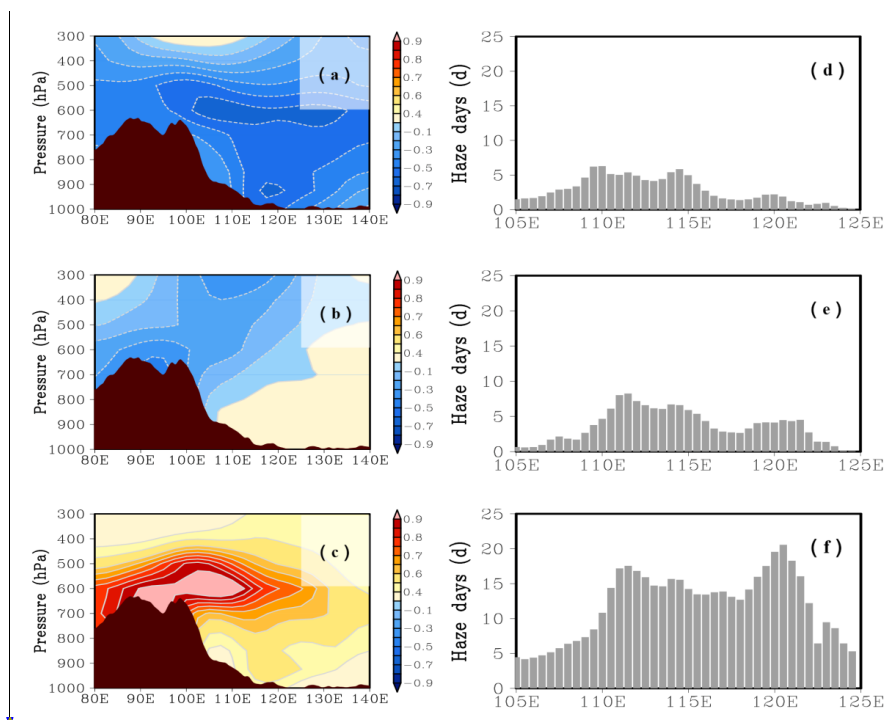


**Figure 4.** Vertical cross sections of (a-c) air temperature anomalies (unit: °C) and (d-f) the number of haze days averaged along 25-40°N in winter during 1961-1980 (a, d), 1981-2000 (b, e) and 2001-2018 (c, f).

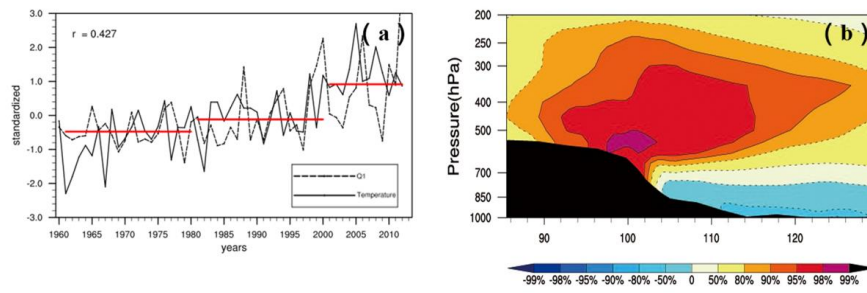


**Figure 5.** (a) Interannual variations of TP's apparent heat source ( $Q_1$ ) and air temperature of meteorological stations in the TP with the altitudes above 3000 meters in the winters during 1960-2014; (b) Vertical cross sections of the correlations between TP's apparent heat ( $Q_1$ ) and air temperature latitude-averaged along 30-35°N in the winters during 1960-2014.

#### 4 Conclusions and discussion

Based on the study of the Great Smog of London in 1952 and Beijing's heavy air pollution in 2014, as well

删除的内容:

带格式的: 字体: Times New Roman, 小五

带格式的: 字体: Times New Roman, 小五

删除的内容: C

删除的内容: three decadal periods

删除的内容: TP's apparent heat source ( $Q_1$ ) and air temperature variations.

删除的内容: (a) I

删除的内容: C

删除的内容:

425 as PM<sub>2.5</sub> pollution over EC, the anomalous ‘warm cover’ in the middle troposphere was identified as a  
426 precursory ‘strong signal’ for severe air pollution events, which could be attributed to climate change. A  
427 stable thermal structure in the middle troposphere, i.e. a ‘warm cover’, suppressed the ABL development,  
428 which was a key ‘inducement’ for the accumulation of air pollutants in the ambient atmosphere.

删除的内容: free

删除的内容:

删除的内容: atmospheric

删除的内容: atmospheric boundary layer

删除的内容: (ABL)

429 From the perspective of the thermal vertical structure in the troposphere, the abnormal vertical  
430 structure in the troposphere during heavy air pollution were understood in this study. The thermal structure  
431 formed by the conventional decline rate of atmospheric air temperature often ‘covers up’ the anomalous  
432 ‘strong signal’ of the troposphere in air pollution process, such as the abnormal stable structure with the  
433 middle warm and bottom cold in the troposphere with air temperature anomalies. The ‘strong signal’ of the  
434 ‘warm cover’ of air temperature anomalies in the middle troposphere during heavy air pollution can be  
435 described by the method of statistical comprehensive diagnosis analysis.

436 A large-scale anomalous air temperature pattern of ‘upper warming and bottom cooling’ in the  
437 troposphere appeared from the TP to the downstream EC region and even the entire East Asian region. The  
438 frequent haze pollution events in EC since the start of the 21st century happens to be within a significant  
439 positive phase in the interdecadal variations of ‘warm cover’ in the middle troposphere. A close relationship  
440 between the TP’s heat and the thermal structure in the atmosphere in EC and even the entire East Asian  
441 region reflected an important role of TP’s thermal forcing in environment change over China.

删除的内容:

删除的内容: middle

删除的内容: plateau

删除的内容: plateau

442 ▲ 带格式的: 字体: 五号

443 *Data availability.* The monthly NCEP/NCAR reanalysis data of meteorology are collected from the U.S.  
444 National Center for Environmental Protection (NCEP, <https://www.esrl.noaa.gov/>); the daily and monthly  
445 ERA-Interim reanalysis data of meteorology are collected from the European Center for Medium-range  
446 Weather Forecasts (ECMWF, <https://www.ecmwf.int/>); the hourly PM<sub>2.5</sub> concentration data are collected

457 from the national air quality monitoring network operated by the Ministry of Ecology and Environment [the](#)  
458 [People's Republic](#) of China (<http://www.mee.gov.cn/>); the air temperature of surface observation data and  
459 L-band sounding data are obtained from the China Meteorological Information Center (<http://data.cma.cn/>).

删除的内容: <http://cdc.cma.gov.cn/>

460 All data presented in this paper are available upon request to the corresponding author (Wenyue Cai,  
461 [caiwy@cma.gov.cn](mailto:caiwy@cma.gov.cn)).

462

463 *Author contributions.* XDX and WYC designed the study. XDX, WYC and TLZ performed the research.  
464 WYC performed the statistical analyses. XDX, WYC and TLZ wrote the initial paper. TLZ, XFX, WHZ,  
465 CS, PY, CZW and FG contributed to subsequent revisions.

删除的内容: and

466

467 *Competing interests.* The authors declare that they have no conflict of interest.

468

469 *Acknowledgements.* This study is supported by the Atmospheric Pollution Control of the Prime Minister  
470 Fund (DQGG0104), the National Natural Science Foundation of China (91644223) and the Second Tibet  
471 Plateau Scientific Expedition and Research program (STEP, 2019QZKK0105).

472

473 *Financial support.* This research has been supported by the Atmospheric Pollution Control of the Prime  
474 Minister Fund (DQGG0104), the National Natural Science Foundation of China (91644223) and the  
475 Second Tibet Plateau Scientific Expedition and Research program (STEP, 2019QZKK0105).

476

## 477 **References**

478 Cai, M., OU, J. J., Zhou, Y. Q., Yang Q., and Cai, Z. X.: Discriminating cloud area by using L-band  
479 sounding data [\(in Chinese\)](#), Chin. J. Atmos. Sci., 38, 213–222,  
480 <https://doi.org/10.3878/j.issn.1006-9895.2013.12193>, 2014.

483 Cai, W. Y., Xu, X. D., Cheng, X. H., Wei, F. Y., Qiu, X. F., and Zhu, W. H.: Impact of “blocking” structure  
484 in the troposphere on the wintertime persistent heavy air pollution in northern China, *Sci. Total*  
485 *Environ.*, 741, 140325, <https://doi.org/10.1016/j.scitotenv.2020.140325>, 2020.

486 Cheng, Y. F., Zheng, G. J., Wei, C., Mu, Q., Zheng, B., Wang, Z. B., Gao, M., Zhang, Q., He, K. B.,  
487 Carmichael, G., Poschl, U., and Su, H.: Reactive nitrogen chemistry in aerosol water as a source of  
488 sulfate during haze events in China, *Sci. Adv.*, 2, e1601530, <https://doi.org/10.1126/sciadv.1601530>,  
489 2016.

490 China Ministry of Environmental Protection: Technical Regulation on Ambient Air Quality Index (On Trial)  
491 (HJ633-2012), China Environmental Science Press, Beijing, China, 2012.

492 Ding, Y. H. and Liu, Y. J.: Analysis of long-term variations of fog and haze in China in recent 50 years and  
493 their relations with atmospheric humidity, *Science China: Earth Sciences*, 57, 36-46,  
494 <https://doi.org/10.1007/s11430-013-4792-1>, 2014.

495 Huang, R. J., Zhang, Y., Bozzetti, C., Ho, K. F., Cao, J. J., Han, Y. M., Daellenbach, K. R., Slowik, J. G.,  
496 Platt, S. M., Canonaco, F., Zotter, P., Wolf, R., Pieber, S. M., Bruns, E. A., Crippa, M., Ciarelli, G.,  
497 Piazzalunga, A., Schwikowski, M., Abbaszade, G., Schnelle-Kreis, J., Zimmermann, R., An, Z. S.,  
498 Szidat, S., Baltensperger, U., Haddad, I. E., 11, and Prevot, A-S. H.: High secondary aerosol  
499 contribution to particulate pollution during haze events in China, *Nature*, 514, 218–222,  
500 <https://doi.org/10.1038/nature13774>, 2014.

501 Li, W., Li, F., Zhao, Z. Q., Liu, F. Q., Li, B., Li, H.: L-Band Meteorological Observation System  
502 Construction Technology Assessment Report (in Chinese), China Meteorological Press, Beijing, China,  
503 2009.

504 Liu, S. Y. and Liang, Z. X.: Observed diurnal cycle climatology of planetary boundary layer height, *J.*  
505 *Climate*, 23, 5790-5809, <https://doi.org/10.1175/2010JCLI3552.1>, 2010.

506 [Miao, Y. C., Li, J., Miao, S. G., Che, H. Z., Wang, Y. Q., Zhang, X. Y., Zhu, R., and Liu, S. H.: Interaction](#)  
507 [Between Planetary Boundary Layer and PM<sub>2.5</sub> Pollution in Megacities in China: a Review. \*Current\*](#)  
508 [Pollution Reports](#), 5, 261–271, <https://doi.org/10.1007/s40726-019-00124-5>, 2019.

509 [Quan, J. N., Gao, Y., Zhang, Q., Tie, X. X., Cao, J. J., Han, S. Q., Meng, J. W., Chen, P. F., and Zhao, D. L.:](#)  
510 [Evolution of planetary boundary layer under different weather conditions, and its impact on aerosol](#)  
511 [concentrations, \*Particuology\*, 11\(1\), 34-40, <https://doi.org/10.1016/j.partic.2012.04.005>, 2013.](#)

512 [Quan, J. N., Xu, X. D., Jia, X. C., Liu, S. H., Miao, S. G., Xin, J. Y., Hu, F., Wang, Z. F., Fan, S. J., Zhang,](#)  
513 [H. S., Mu, Y. J., Dou, Y. W., and Cheng, Z.: Multi-scale processes in severe haze events in China and](#)  
514 [their interactions with aerosols: Mechanisms and progresses \(in Chinese\), \*Chin Sci Bull\*, 65, 810–824,](#)  
515 <https://doi.org/10.1360/TB-2019-0197>, 2020.

516 [State Council of the People’s Republic of China: Notice of the General Office of the State Council on](#)  
517 [Issuing the Air Pollution Prevention and Control Action Plan, State Council of the People’s Republic](#)  
518 [of China website. Available at: \[http://www.gov.cn/zwgk/2013-09/12/content\\\_2486773.htm\]\(http://www.gov.cn/zwgk/2013-09/12/content\_2486773.htm\), 2013.](#)

519 [State Council of the People’s Republic of China: Notice of the General Office of the State Council on](#)  
520 [Issuing the Air Pollution Prevention and Control Action Plan, State Council of the People’s Republic](#)  
521 [of China website. Available at: \[http://www.gov.cn/zhengce/content/2018-07/03/content\\\_5303158.htm\]\(http://www.gov.cn/zhengce/content/2018-07/03/content\_5303158.htm\),](#)  
522 [2018.](#)

523 Tan, C. H., Zhao, T. L., Cui, C. G., Luo, B. L., and Bai, Y. Q.: Characterization of haze pollution over  
524 Central China during the past 50 years, *Science in China (in Chinese)*, *China Environ. Sci.*, 35, 2272–  
525 2280, 2015.

526 Tang, G. Q., Zhang, J. Q., Zhu, X. W., Tao, S., Munkel, C., Hu, B., Schaefer, K., Liu, Z. R., Zhang, J. K.,  
527 Wang, L. L., Xin, J. Y., Schaefer, P., and Wang, Y. S.: Mixing layer height and its implications for air  
528 pollution over Beijing, China, *Atmos. Chem. Phys.*, 16, 2459–2475,  
529 <https://doi.org/10.5194/acp-16-2459-2016>, 2016.

530 Tie, X. X. and Cao, J. J.: Aerosol pollutions in eastern China: Present and future impacts on environment,  
531 *Particuology*, 7, 426–431, <https://doi.org/10.1016/j.partic.2009.09.003>, 2009.

532 Wang, G. H., Zhang, R. Y., Gomez, M. E., Yang, L. X., Zamora, M. L., Hu, M., Lin, Y., Peng, J. F., Guo, S.,



533 Meng, J. J., Li, J. J., Cheng, C. L., Hu, T. F., Ren, Y. Q., Wang, Y. S., Gao, J., Cao, J. J., An, Z. S.,  
534 Zhou, W. J., Li, G. H., Wang, J. Y., Tian, P. F., Marrero-Ortiz, W., Secrest, J., Du, Z. F., Zheng, J.,  
535 Shang, D. J., Zeng, L. M., Shao, M., Wang, W. G., Huang, Y., Wang, Y., Zhu, Y. J., Li, Y. X., Hu, J. X.,  
536 Pan, B., Cai, L., Cheng, Y. T., Ji, Y. M., Zhang, F., Rosenfeld, D., Liss, P. S., Duce, R. A., Kolb, C. E.,  
537 and Molina, M. J.: Persistent sulfate formation from London Fog to Chinese Haze, *P. Natl. Acad. Sci.*,  
538 113, 13630–13635, <https://doi.org/10.1073/pnas.1616540113>, 2016.

539 Wang, H., Li, J. H., Peng, Y., Zhang, M., Che, H. Z., and Zhang, X. Y.: The impacts of the meteorology  
540 features on PM<sub>2.5</sub> levels during a severe haze episode in central-east China, *Atmospheric Environment*,  
541 197, 177–189, <https://doi.org/10.1016/j.atmosenv.2018.10.001>, 2019.

542 Wang, H., Xue, M., Zhang, X. Y., Liu, H. L., Zhou, C. H., Tan, S. C., Che, H. Z., Chen, B., and Li, T.:  
543 Mesoscale modeling study of the interactions between aerosols and PBL meteorology during a haze  
544 episode in Jing–Jin–Ji (China) and its nearby surrounding region – Part 1: Aerosol distributions and  
545 meteorological features, *Atmos. Chem. Phys.*, 15, 3257–3275,  
546 <https://doi.org/10.5194/acp-15-3257-2015>, 2015.

547 Wang, J. J., Zhang, M. G., Bai, X. L., Tan, H. J., Li, S., Liu, J. P., Zhang, R., Wolters, M. A., Qin, X. Y.,  
548 Zhang, M. M., Lin, H. M., Li, Y. N., Li, J., and Chen, L. Q.: Large-scale transport of PM<sub>2.5</sub> in the  
549 lower troposphere during winter cold surges in China, *Sci. Rep.*, 7, 13238,  
550 <https://doi.org/10.1038/s41598-017-13217-2>, 2017.

551 [Wang, Y. S., Li, W. J., Gao, W. K., Liu, Z. R., Tian, S. L., Shen, R. R., Ji, D. S., Wang, S., Wang, L. L.,](#)  
552 [Tang, G. Q., Song, T., Cheng, M. T., Wang, G. H., Gong, Z. Y., Hao, J. M., and Zhang, Y. H.: Trends in](#)  
553 [particulate matter and its chemical compositions in China from 2013–2017. \*Science China Earth\*](#)  
554 [Sciences, 62: 1857–1871, <https://doi.org/10.1007/s11430-018-9373-1>, 2019.](#)

555 Whittaker, A., Berube, K., Jones, T., Maynard, R., Richards, R.: Killer smog of London, 50 years on:  
556 particle properties and oxidative capacity, *Science of the Total Environment*, 334–335, 435–445,  
557 <https://doi.org/10.1016/j.scitotenv.2004.04.047>, 2004.

558 [Xu, X. D., Zhao, T. L., Liu, F., Gong, S. L., Kristovich, D., Lu, C., Guo, Y., Cheng, X. H., Wang, Y. J., and](#)  
559 [Ding, G.: Climate modulation of the Tibetan Plateau on haze in China. \*Atmos. Chem. Phys.\*, 16, 1365–](#)  
560 [1375, <https://doi.org/10.5194/acp-16-1365-2016>, 2016.](#)

561 Yim, S-Y., Wang, B., Liu, J., and Wu, Z. W.: A comparison of regional monsoon variability using monsoon  
562 indices, *Climate Dynamics*, 43, 1423–1437, <https://doi.org/10.1007/s00382-013-1956-9>, 2014.

563 Zhang, X. Y., Wang, J. Z., Wang, Y. Q., Liu, H. L., Sun, J. Y., and Zhang, Y. M.: Changes in chemical  
564 components of aerosol particles in different haze regions in China from 2006 to 2013 and contribution  
565 of meteorological factors, *Atmos. Chem. Phys.*, 15, 12935–12952,  
566 <https://doi.org/10.5194/acp-15-12935-2015>, 2015.

567 Zhu, W. H., Xu, X. D., Zheng, J., Yan, P., Wang, Y. J., and Cai, W. Y.: The characteristics of abnormal  
568 wintertime pollution events in the Jing-Jin-Ji region and its relationships with meteorological factors,  
569 *Sci. Total Environ.*, 626, 887-898, <https://doi.org/10.1016/j.scitotenv.2018.01.083>, 2018.